Energy Internet

WILEY

ORIGINAL RESEARCH OPEN ACCESS

Towards Continuous-Time Safe Energy Management in Shared Renewables and Refined Oil Transmission Systems

Shengshi Wang[1,2] | Danji Huang[3] | Jiakun Fang[1] | Xiaomeng Ai[1] | Shichang Cui[1] | Miao Li[4] | Ge Yan[4] | Kun Mei[5] | Sen Li[4] | Qicong Liu[5] | Hao Li[5]

[1]State Key Laboratory of Advanced Electromagnetic Technology, School of Electrical and Electronic Engineering, Huazhong University of Science and Technology, Wuhan, China | [2]School of Engineering, Cardiff University, Cardiff, UK | [3]PetroChina ShenZhen New Energy Research Institute Co., Ltd., Shenzhen, China | [4]PipeChina South China Company, Guangzhou, China | [5]CET Electric Technology Inc., Shenzhen, China

Correspondence: Jiakun Fang (jfa@hust.edu.cn)

Received: 22 August 2024 | **Revised:** 14 January 2025 | **Accepted:** 28 January 2025

Funding: This work was supported by the National Natural Science Foundation of China 52177089, the Fundamental Research Funds for the Central Universities YCJJ20230463, and PipeChina South China Company GWHT20200001399.

Keywords: continuous-time model | energy transition | physics-informed particle swarm optimization | safe energy management | shared renewables and refined oil transmission system

ABSTRACT

This paper investigates the safe energy management of emerging shared renewables and refined oil transmission systems (SRROTSs) during the energy transition. Specifically, a continuous-time energy management model that considers the SRROTSs' multi-product sequential transmission characteristics is proposed to guide safe and efficient system operation. This model is also convenient for on-site dispatchers to operate. Correspondingly, a solver-free physics-informed particle swarm optimisation (PI-PSO) algorithm is tailored, utilising physical rules to regulate particle mutation and adapted to solve the proposed model, thereby enhancing the optimality and stability of the solution. Case studies on real-world SRROTSs are utilised to validate the proposed model and PI-PSO algorithm, which are expected to be generalised to other pipeline transmission systems. Especially, the PI-PSO algorithm achieves a 25.6% energy reduction compared to the original PSO algorithm, although a trade-off between improving the objective value and the number of iterations needed for convergence is observed.

1 | Introduction

Since the Industrial Revolution, human activities have significantly increased the release of carbon dioxide (CO_2) into the atmosphere due to the consumption of fossil fuels, with global carbon emissions rising from 8.9 $GtCO_2$ in 1959 [1] to 35.8 $GtCO_2$ in 2023 [2]. Accordingly, this leads to climate change, manifesting as global warming, extreme weather events, and other adverse effects, which threaten people's livelihoods. Hence, energy transition to reduce greenhouse gas emissions is urgently needed.

One promising approach for greenhouse gas reduction is to substitute traditional fossil fuels, such as refined oil and natural gas, with their renewable alternatives, such as biofuels and hydrogen [3, 4]. In many cases, such as in China, renewable energy production sites are often located far from load centres, typically in regions rich in solar or wind resources [5]. This makes efficient energy transmission crucial. However, constructing infrastructure such as transmission pipelines for these renewables requires significant investment and a long period before the capital is reimbursed [3]. Hence, it is natural to utilise the remaining capacity of existing energy transmission infrastructures, especially when their loads remain stable without significant growth or even in a downward trend due to the diversification of transmission modes as well as the increased utilisation of clean energy [6]. Accordingly, this paper focuses

Abbreviations: IS, initial station; LS, local station; PI-PSO, physics-informed particle swarm optimisation; SRROTS, shared renewables and refined oil transmission systems; TS, terminal station.

This is an open access article under the terms of the Creative Commons Attribution-NonCommercial-NoDerivs License, which permits use and distribution in any medium, provided the original work is properly cited, the use is non-commercial and no modifications or adaptations are made.

© 2025 The Author(s). *Energy Internet* published by John Wiley & Sons Ltd on behalf of ©The IET + Chinese Society of Electrical Engineering (CSEE).

on the emerging shared renewables and refined oil transmission systems (SRROTSs), which sequentially transmit refined oil and renewable fuels that have physicochemical similarities [3, 6], functioning as multi-product pipelines [7], which consume approximately 45 TWh of electricity globally each year [8]. Herein, we particularly emphasise their energy management as well as security.

The aim of the energy management of SRROTSs is to safely operate the system with the minimal operational energy consumption [9]. It includes the batch delivery scheduling, electric pump scheduling and chemical drag reducer injection planning [10, 11]. In ref. [8], a distributed pump scheduling method of SRROTSs is proposed to reach quasi-optimality preservation under uncertainty. In ref. [12], the batch delivery and electric pump scheduling are considered in the optimal bidding strategy problem of SRROTSs to participate within electricity and pipeline logistics markets. Tu et al. [13] estimate the remaining capacity of multi-product pipelines for renewable fuels through energy management of SRROTSs. In ref. [14], the energy management objective is incorporated into the design stage of SRROTSs. In this paper, we particularly concentrate on addressing the urgent needs of dispatchers, specifically the electric pump scheduling of SRROTSs. The goal is to provide practical support for their daily operations by achieving secure and accurate pump scheduling results. This involves minimising electric energy consumption to the largest extent, thereby enhancing the efficiency and practicality of the scheduling process.

Traditionally, the energy management model for the multi-product pipelines evenly divides the scheduling horizon into discrete time-steps and is solved by the solvers [15]. However, it faces a dilemma between solution time and accuracy [16]. Too many divisions lead to solving and operational difficulties, while too few divisions can cause model distortion, resulting in energy waste and potential safety issues. With the emergence of continuous-time energy management, the changing trajectories of the system status over the entire time horizon can be precisely evaluated [17, 18]. In this approach, the system's actions can occur at any moment, unrestricted by predefined time-steps, thereby allowing for greater flexibility and safety. In ref. [19], the function-space optimisation is utilised to coordinate the integrated natural gas and power system. As an extension, Zheng et al. [20] propose the multi-energy analysis in both continuous time and space. Furthermore, Zhou et al. [21] enhance the accuracy of characterising the system's continuous-time behaviour. To summarise, researchers focusing on continuous-time energy management emphasise gaining insights into the mathematical expressions of the system's physical properties and establishing specific adaptive models. Hence, for SRROTSs, the multi-product sequential transmission characteristics must be considered to guide the establishment of a continuous-time energy management model for operational safety and efficiency.

Beyond operational safety, potential cyber issues in energy transitions, which can disrupt the energy supply chain, have significant implications for a nation's security posture [22], and as a result, they have expanded the scope of energy security [23]. Typically, solvers are employed for solving energy system optimisation [10, 24]. In ref. [25], a mixed-integer linear programming approach is developed for power system dispatch and solved using a solver. In ref. [26], the nonconvex branch flow model for a hybrid AC/DC power grid is relaxed into a second-order cone programming form and directly solved by a solver. Cafaro et al. [27] introduce mixed-integer nonlinear programming for the scheduling of refined product pipelines and proposes a master-slave framework that combines a solver with an iterative procedure. However, for backbone energy infrastructure companies, the main task is to guarantee robust energy transmission. Solvers, especially those from abroad, might bring them concerns about those potential issues. Metaheuristic algorithms offer an upgrade by balancing global and regional searches, making them promising for nonconvex optimisation [28]. Additionally, they are also solver-free, providing a safer option for backbone energy infrastructure companies.

Overall, the main challenges include: (1) **Continuous-Time Energy Management Characterisation:** Establishing a continuous-time model based on the multi-product sequential transmission feature of SRROTSs to ensure operational safety and efficiency; (2) **Time-Varying Parameters Handling:** Developing methods to effectively manage parameters that change with time, which is crucial for maintaining model accuracy and reliability; (3) **High-Performance Solution Algorithm Development:** Finding ways to solve the model with good stability, while balancing solution optimality and solving time, which is essential for practical and efficient application. Accordingly, this paper proposes a continuous-time optimal energy management model motivated by the emergence of SRROTSs in energy transition and the need for safe energy management. A corresponding solution technique is also designed and adapted. Challenges related to two key energy security issues: operational safety and cyber issues are both addressed. The main contributions are as follows, compared with other studies in Table 1.

1. We explore the energy management issues of the emerging SRROTSs in the energy transition, focusing on making them low-carbon and ensuring their security. For safe and efficient system operation, we propose a continuous-time energy management model that considers the SRROTSs' multi-product sequential transmission characteristics. The core idea is to treat the time division points as adjustable "sliders" throughout the entire scheduling horizon of interest. It is also convenient for the on-site dispatchers to operate.
2. For potential cyber issues and also to solve the proposed model, we especially tailor a solver-free physics-informed particle swarm optimisation (PI-PSO) algorithm, utilising physical rules to regulate particle mutation, thereby enhancing the optimality and stability of the solution.
3. The proposed model and algorithm are validated with real-world SRROTSs, and expected to be generalised to other pipeline transmission systems.

The rest of the paper is organised as follows: Section 2 introduces SRROTSs' physical characteristics and defines the problem addressed in this paper. Section 3 describes the proposed model, and Section 4 details the corresponding solution

29952166, 0, Downloaded from https://ietresearch.onlinelibrary.wiley.com/doi/10.1049/ein2.12024 by Welsh Assembly Government, Wiley Online Library on [06/05/2025]. See the Terms and Conditions (https://onlinelibrary.wiley.com/terms-and-conditions) on Wiley Online Library for rules of use; OA articles are governed by the applicable Creative Commons License

algorithm. Numerical case studies are presented in Section 5, and conclusions are drawn in Section 6.

2 | Problem Description

The emerging SRROTSs, as shown in Figure 1, facilitate the transportation of both refined oil products and renewable alternatives in sequences within existing cross-regional pipeline infrastructures. In this system, traditional fossil fuels are partially substituted with renewables, leading to cleaner energy usage. Starting from the initial station (IS), the liquids are loaded and propelled forward by electric pumps located at various local stations (LSs) along the pipeline to the terminal station (TS). Based on local transmission demand, the dispatch centre determines the batch schedule and pump operations, then communicates these instructions to the local stations.

Specifically, this paper focuses on the optimal energy management of SRROTSs given the sequential transmission schedule. The traditional approach to model establishment involves manually dividing the time horizon into equal time-steps, followed by solving the model using solvers. However, this can cause safety issues, that is, operational safety and privacy safety. For operational safety, as illustrated in Figure 2, when the pressure drop, an essential model parameter, changes within a time-step, the equally divided time-steps (t_1 and t_2 in Figure 2) may overlook this variation (as shown by the imaginary pressure drop in Figure 2), potentially causing the pressure to fall into an unsecure region. Instead, we aim to identify the precise time points (t_1' in Figure 2) for pump startups and shutdowns based on the system's physical characteristics. This ensures that only monotonic changes occur within the divided time intervals. Accordingly, also for privacy safety, the solution technique will be designed to meet this requirement while reducing the use of solvers to protect energy security.

3 | Mathematical Model

3.1 | Pre-Division of the Time-Steps

In the traditional model, time-steps are divided equally. However, in this paper, the time horizon is pre-divided into unequal time-steps according to the sequential transmission characteristics in SRROTSs. In Figure 3, we consider that multiple

TABLE 1 | Comparison of research on energy management schemes for SRROTSs.

Reference	Multi-products	Rigorous physical description	Continuous-time representation	Solution technique
[4]	Hydrogen and natural gas	Yes	No	Mixed integer nonlinear programming
[6, 14]	Renewable fuels and refined oil	No	No	Mixed integer linear programming
[3, 8, 11, 12]	Renewable fuels and refined oil	Yes	No	Mixed integer linear programming
[7, 10, 13, 15]	Refined oil	Yes	No	Mixed integer linear programming
[30]	Refined oil	Yes	No	Mixed integer nonlinear programming
This paper	Renewable fuels and refined oil	Yes	Yes	Physics-informed metaheuristic

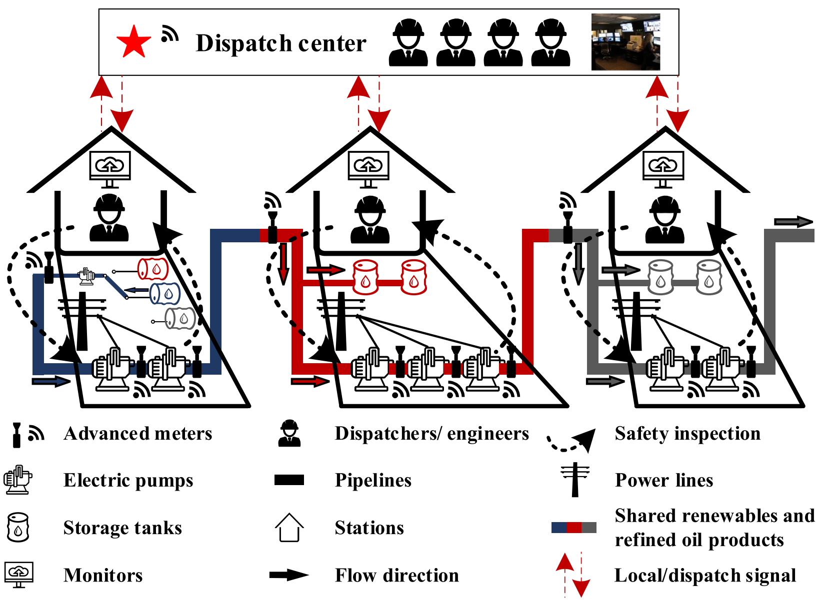

FIGURE 1 | The sketch map of SRROTSs.

29952166, 0, Downloaded from https://ietresearch.onlinelibrary.wiley.com/doi/10.1049/ein2.12024 by Welsh Assembly Government, Wiley Online Library on [06/05/2025]. See the Terms and Conditions (https://onlinelibrary.wiley.com/terms-and-conditions) on Wiley Online Library for rules of use; OA articles are governed by the applicable Creative Commons License

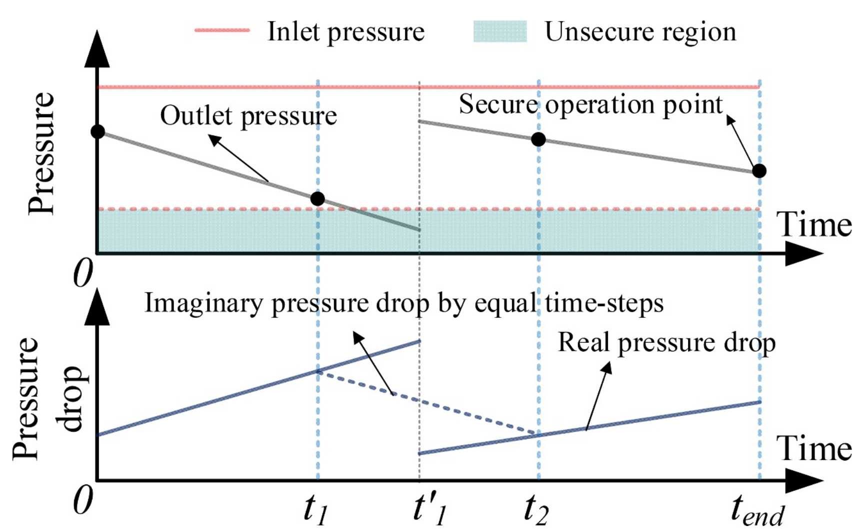

FIGURE 2 | Safety issue of equal time-steps.

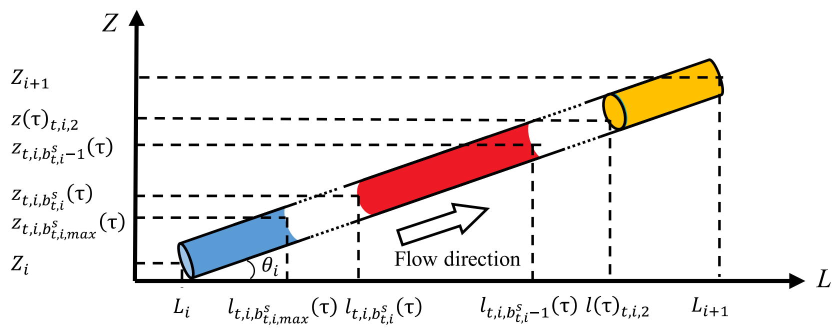

FIGURE 3 | An illustrative pipeline segment with multiple batches.

batches exist in a pipeline segment $(i, i+1)$ at the start time of a time-step t. Correspondingly, the pressure drop $P^{drop}_{t,i}$ can be analytically calculated by Darcy–Weisbach equation [29]:

$$P^{\text{drop}}_{t,i,1}(\tau) = \rho_{t,i,1}(L_{i+1} - l_{t,i,2}(\tau))\lambda_{t,i,1}\frac{8\left(Q^{\text{segment}}_{t,i}\right)^2}{\pi^2 D_i{}^5 \cos\theta_i} + \rho_{t,i,1}g(Z_{i+1} - z_{t,i,2}(\tau)),\ i < i_{\max} \quad (1)$$

$$P^{\text{drop}}_{t,i,b^s_{t,i,\max}}(\tau) = \rho_{t,i,b^s_{t,i,\max}}\left(l_{t,i,b^s_{t,i,\max}}(\tau) - L_i\right)\lambda_{t,i,b^s_{t,i,\max}}\frac{8\left(Q^{\text{segment}}_{t,i}\right)^2}{\pi^2 D_i{}^5 \cos\theta_i} + \rho_{t,i,b^s_{t,i,\max}}g\left(z_{t,i,b^s_{t,i,\max}}(\tau) - Z_i\right),\ i < i_{\max} \quad (2)$$

$$P^{\text{drop}}_{t,i,b^s_{t,i}}(\tau) = \rho_{t,i,b^s_{t,i,\max}}\left(l_{t,i,b^s_{t,i}}(\tau) - l_{t,i,b^s_{t,i}+1}(\tau)\right)\lambda_{t,i,b^s_{t,i,\max}} \times \frac{8\left(Q^{\text{segment}}_{t,i}\right)^2}{\pi^2 D_i{}^5 \cos\theta_i} + \rho_{t,i,b^s_{t,i,\max}}g\left(z_{t,i,b^s_{t,i}}(\tau) - z_{t,i,b^s_{t,i}+1}(\tau)\right), \times 1 < b^s_{t,i} < b^s_{t,i.\max},\ i < i_{\max} \quad (3)$$

where $P^{\text{drop}}_{t,i,b^s_{t,i}}(\tau)$ is the pressure drop of batch $b^s_{t,i}$ at time τ in pipeline segment $(i, i+1)$ during time-step t; $l(\tau)$ and $z(\tau)$ refer to the horizontal coordinate and elevation of the interface of batch $b^s_{t,i}$ and batch $b^s_{t,i} - 1$ in pipeline segment $(i, i+1)$ at time τ, respectively. $l(\tau)$ and $z(\tau)$ can be calculated as follows:

$$l_{t,i,b^s_{t,i}}(\tau) = l_{t,i,b^s_{t,i}}(0) + \frac{\int_0^\tau Q^{\text{segment}}_{t,i}d\tau}{A_i}\cos\theta_i,\ b^s_{t,i} > 1,\ i < i_{\max} \quad (4)$$

$$z_{t,i,b^s_{t,i}}(\tau) = z_{t,i,b^s_{t,i}}(0) + \frac{\int_0^\tau Q^{\text{segment}}_{t,i}d\tau}{A_i}\sin\theta_i,\ b^s_{t,i} > 1,\ i < i_{\max} \quad (5)$$

where A_i is the cross-sectional area of pipeline segment $(i, i+1)$, and $l_{t,i,b^s_{t,i}}(0)$ as well as $z_{t,i,b^s_{t,i}}(0)$ are the horizontal and vertical positions of the interface at the start time of time-step t, respectively.

If the flow rate $Q^{\text{segment}}_{t,i}$ and batch information (i.e., type and sequence order of liquid products) for pipeline segments do not change, there will be no batch flow in or out of any pipeline segments. Hence, $l(\tau)$ and $z(\tau)$ change linearly with time, as does the total pressure drop $P^{\text{drop}}_{t,i}$:

$$P^{\text{drop}}_{t,i}(\tau) = \sum_{b^s_{t,i} \in B^s_{t,i}} P^{drop}_{t,i,b^s_{t,i}}(\tau) = \alpha_{t,i}t + \beta_{t,i},\ i < i_{\max} \quad (6)$$

29952166, 0, Downloaded from https://ietresearch.onlinelibrary.wiley.com/doi/10.1049/ein2.12024 by Welsh Assembly Government, Wiley Online Library on [06/05/2025]. See the Terms and Conditions (https://onlinelibrary.wiley.com/terms-and-conditions) on Wiley Online Library for rules of use; OA articles are governed by the applicable Creative Commons License

Hence, the time interval during which the flow rate and batch information for all pipeline segments remain unchanged can be considered a pre-divided time step, wherein the operational parameters of the SRROTS change monotonous with time.

3.2 | Post-Division of the Time-Steps: The Idea of Continuous-Time Optimal Energy Management in SRROTSs

Traditionally, the pump status to be determined remains constant [30] within the equally pre-divided time-steps. However, in the proposed continuous-time energy management model, the precise startup and shutdown times of the pumps are treated as adjustable 'sliders' (i.e., the pump working time zone in Figure 4) throughout the entire scheduling horizon. Hence, the status of the pumps within a pre-divided time step is not fixed. Specifically, we determine the pumps' startup and shutdown times along the time axis and subsequently examine the pressure distribution along the pipeline using hydraulic equations to ensure it remains within the safety region throughout the entire scheduling horizon. Particularly, as shown in Figure 4, the pressure drop value at the post-divided time points can be interpolated thanks to its linear property. If the pressure exceeds the upper limit or drops below the lower limit, the current positions of the "sliders" are deemed infeasible and will be updated according to a certain rule. Note that multiple iterations are required to obtain a practical solution. During each iteration, the time horizon is further divided into more time steps based on the pre-divided ones, according to the determined pump operating time zones. These post-divided time steps are the ones considered in our proposed model. The detailed iteration process will later be introduced in Section 4.3.

3.3 | Constraints

With the post-divided time-steps and pump working time zone, the constraints aim to detailly examine the safety of SRROTS operation.

3.3.1 | Energy Balance

$$P_{t,i}^{\text{station}} = \sum_{k \in K_i} SP_{t,i,k}\rho_{t,i} g H_{t,i,k} \tag{7}$$

$$POUT_{t,i} = \text{PIN}_{t,i} + P_{t,i}^{\text{station}},\ i < i_{\max} \tag{8}$$

$$PO_{t,i} = PI_{t,i} + PH_{t,i} \tag{9}$$

$$\text{PIN}_{t,i+1} = \text{POUT}_{t,i} - P_{t,i}^{\text{drop}}(0) \quad i < i_{\max} \tag{10}$$

$$PI_{t,i+1} = PO_{t,i} - \left(\alpha_{t,i} TP_t + P_{t,i}^{\text{drop}}(0)\right) \tag{11}$$

$$\text{PIN}_{t,1} = PI_{t,1} = P_t^f \tag{12}$$

$$\text{PIN}_{\min} - \delta_{t,i,\min}^{\text{pressure},1} \le \text{PIN}_{t,i} \le \text{PIN}_{\max} + \delta_{t,i,\max}^{\text{pressure},1} \tag{13}$$

$$POUT_{\min} - \delta_{t,i,\min}^{\text{pressure},2} \le POUT_{t,i} \le POUT_{\max} + \delta_{t,i,\max}^{\text{pressure},2} \tag{14}$$

$$\text{PIN}_{\min} - \delta_{t,i,\min}^{\text{pressure},3} \le PI_{t,i} \le \text{PIN}_{\max} + \delta_{t,i,\max}^{\text{pressure},3} \tag{15}$$

$$\text{POUT}_{\min} - \delta_{t,i,\min}^{\text{pressure},4} \le PO_{t,i} \le \text{POUT}_{\max} + \delta_{t,i,\max}^{\text{pressure},4} \tag{16}$$

Equation (7) describes the pressure provided by a pump station. In each time-step, the pressure drop changes with time, and thus, we take the inlet and outlet pressure of each station at the end time of time-steps into consideration. The relationship between the inlet and outlet pressures of each station at the start and end times of time-step t is given in Equations (8) and (9), respectively. The inlet pressure of a station equals the outlet pressure of the upstream station minus the pressure drop of the pipeline segment between them

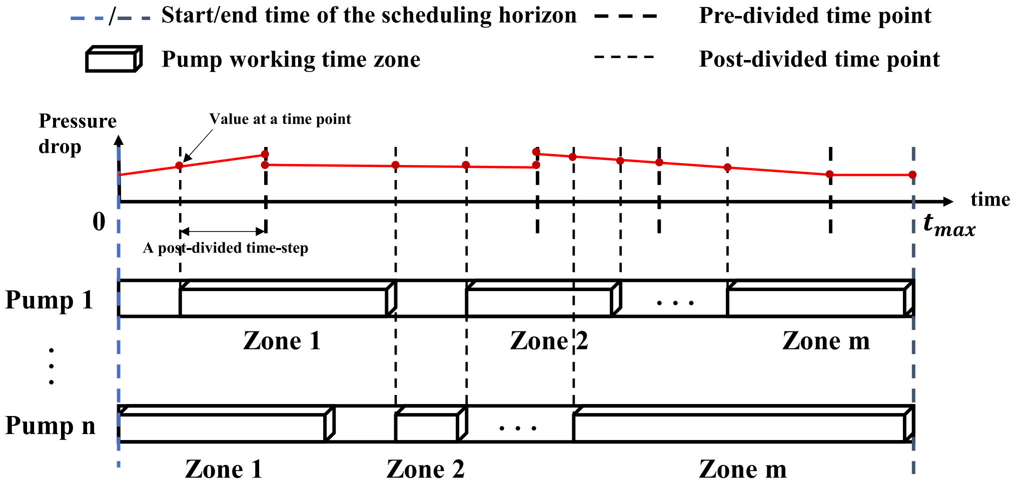

FIGURE 4 | Illustration of the idea of continuous-time optimal energy management in SRROTSs.

29952166, 0, Downloaded from https://ietresearch.onlinelibrary.wiley.com/doi/10.1049/eln2.12024 by Welsh Assembly Government, Wiley Online Library on [06/05/2025]. See the Terms and Conditions (https://onlinelibrary.wiley.com/terms-and-conditions) on Wiley Online Library for rules of use; OA articles are governed by the applicable Creative Commons License

(Equations (10) and (11)). Equation (12) shows the boundary condition of the inlet pressure at the initial station. Equations (13)–(16) explain the pressure safe limit of inlet and outlet pressure at each station. Under normal operating conditions, the inlet and outlet pressures of a station must exceed the normal lower limit and remain within the normal upper limit. For pump stations, the lower limit of the inlet pressure is slightly adjusted to prevent hydraulic cavitation. For the final receiving station along the pipeline, the upper limit of the inlet pressure is lower than the normal upper limit.

3.3.2 | Pump Characteristics

$$H_{t,i,k} = a_{i,k} + b_{i,k}\left(Q_{t,i}^{\text{pump}}\right)^{m_{i,k}} \tag{17}$$

$$\begin{aligned}\eta_{t.i.k} = a_{0i,k} &+ a_{1i,k}\cos\left(\omega_{i,k}Q_{t,i}^{\text{pump}}\right) + b_{1i,k}\sin\left(\omega_{i,k}Q_{t,i}^{\text{pump}}\right)\\ &+ a_{2i,k}\cos\left(2\omega_{i,k}Q_{t,i}^{\text{pump}}\right) + b_{2i,k}\sin\left(2\omega_{i,k}Q_{t,i}^{\text{pump}}\right)\\ &+ a_{3i,k}\cos\left(3\omega_{i,k}Q_{t,i}^{\text{pump}}\right) + b_{3i,k}\sin\left(3\omega_{i,k}Q_{t,i}^{\text{pump}}\right)\end{aligned} \tag{18}$$

$$Q_{t,i,\min}^{\text{pump}} + \left(SP_{t,i,k} - 1\right)M \le Q_{t,i}^{\text{pump}}, \forall k \in K_i \tag{19}$$

$$Q_{t,i,\max}^{\text{pump}} + \left(1 - SP_{t,i,k}\right)M \ge Q_{t,i}^{\text{pump}}, \forall k \in K_i \tag{20}$$

$$SA_{t,i,k} \ge SP_{t,i,k} - SP_{t-1,i,k} \tag{21}$$

$$SA_{t,i,k} \ge SP_{t-1,i,k} - SP_{t,i,k} \tag{22}$$

$$\sum_{\tau=t}^{t'} TP_\tau \ge \left(SP_{t,i,k} + SP_{t',i,k} - 2\right)M + TS_{i,k}, t' \ge t \tag{23}$$

The pumping head and efficiency of each pump can be calculated by fitted curves taking $Q_{i,k}^{\text{pump}}$ as the independent variable, given in Equations (17) and (18). In Equations (19) and (20), the flow rate $Q_{i,k}^{\text{pump}}$ through the pump must meet specific conditions to ensure high-efficiency operation of the pump. Additionally, frequent changes in pump status can result in large currents in the motor, potentially causing damage to the pump. Therefore, frequent pump startups and shutdowns should be avoided, as indicated in Equation (23). This practice also facilitates easier operation for the dispatchers on the industrial site.

3.4 | Objective Function

The objective of optimal energy management in SRROTSs is to minimise total energy consumption during the delivery of liquid products while simultaneously ensuring safe operation. In Equation (24), f_1, $f_{\text{on-off}}$ and f_{safe} represent the total electricity consumption, the penalty associated with pump startup and shutdown, and the penalty of safety issues, respectively.

$$\min Obj = f_1 + f_{\text{on-off}} + f_{\text{safe}} \tag{24}$$

where f_1 is determined by the duration of pump operation and the power of the pump, which depends on the pumping head, density, flow rate of the liquid product through the pump, and pump efficiency. The concrete relationship is described in Equations (25) and (26).

$$f_1 = \sum_t\sum_i\sum_k SP_{t,i,k}P_{t,i,k}TP_t \tag{25}$$

$$P_{t,i,k} = \frac{H_{t,i,k}\rho_{t,i}gQ_{t,i}^{\text{pump}}}{36000\eta_{t.i.k}} \tag{26}$$

The penalty associated with pump startup and shutdown $f_{\text{on-off}}$ is incurred when the status of a pump changes:

$$f_{\text{on-off}} = \sum_t\sum_i\sum_k \text{Pen}^{\text{status}}\text{SA}_{t,i,k} \tag{27}$$

The penalty f_{safe} for safety issues is assessed when the pressure exceeds the safety limits:

$$\begin{aligned}f_{\text{safe}} = &\sum_t\sum_i \text{Pen}^{\text{safe}}\\ &\times\begin{pmatrix}\delta_{t,i,\min}^{\text{pressure},1} + \delta_{t,i,\max}^{\text{pressure},1} + \delta_{t,i,\min}^{\text{pressure},2} + \delta_{t,i,\max}^{\text{pressure},2}\\ + \delta_{t,i,\min}^{\text{pressure},3} + \delta_{t,i,\max}^{\text{pressure},3} + \delta_{t,i,\min}^{\text{pressure},4} + \delta_{t,i,\max}^{\text{pressure},4}\end{pmatrix}\cdot TP_t\end{aligned} \tag{28}$$

4 | Solution Methodology

The classic method for model solving is to use solvers. However, the proposed optimisation model is nonconvex and includes logic equivalence constraints for the post-division of time-steps, which is NP-hard. Therefore, in this paper, we propose the PI-PSO algorithm based on our model, where the startup/shutdown times of the pumps are treated as continuous variables. Once the startup/shutdown times of the pumps are determined, the status of the pumps at all time-steps and the pressure distribution along the pipelines are fixed. Accordingly, the objective function and constraints are utilised to examine the quality of the solutions.

4.1 | Proposed PI-PSO Algorithm

To solve NP-hard problem, the nature inspired PSO algorithm is considered as efficient alternatives, especially when the decision variable is continuous [31]. Briefly, the activities of each

29952166, 0, Downloaded from https://ietresearch.onlinelibrary.wiley.com/doi/10.1049/ein2.12024 by Welsh Assembly Government, Wiley Online Library on [06/05/2025]. See the Terms and Conditions (https://onlinelibrary.wiley.com/terms-and-conditions) on Wiley Online Library for rules of use; OA articles are governed by the applicable Creative Commons License

particle in each iteration of original PSO algorithm are as follows [29]:

1. Calculate the velocity and update the position;
2. Evaluate the value of fitness function according to the current position;
3. Update the best position of the particle according to the fitness function value;
4. Update the best position of the whole particle swarm according to the fitness function value.

In this paper, we incorporate the physical characteristics of the SRROTS to enhance the PSO algorithm, resulting in the proposed PI-PSO algorithm. The PI-PSO algorithm generates and updates the startup and shutdown times of the pumps through physics-informed mutations across iterations, while simultaneously evaluating the pressure distribution along the pipeline. With appropriate pretreatment, parameter initialisation, and physics-informed iterations, the proposed PI-PSO algorithm can ultimately converge to an optimal solution. Its detailed flowchart is shown in Figure 5.

4.2 | Pretreatment and Initialisation

4.2.1 | Data Input and Pre-Division of the Time-Steps

At the pre-division stage, the design and operating parameters of the model, such as the product delivery schedule of the SRROTS, the physical characteristics of the pipeline, and the properties of the liquid products, should first be collected. A typical data sheet from an energy company in China is shown in Figure 6. After extracting and processing the data from this input data sheet, the batch migration chart can be obtained as illustrated in Figure 7. Subsequently, the pre-division of time-steps can be achieved.

4.2.2 | Model Establishing

The objective function and constraints for pump scheduling in the pipeline are established based on the proposed model. This model forms the core of the calculation process. Once the startup and shutdown times of each pump are determined, they can be inserted into the pre-divided time-steps, forming the

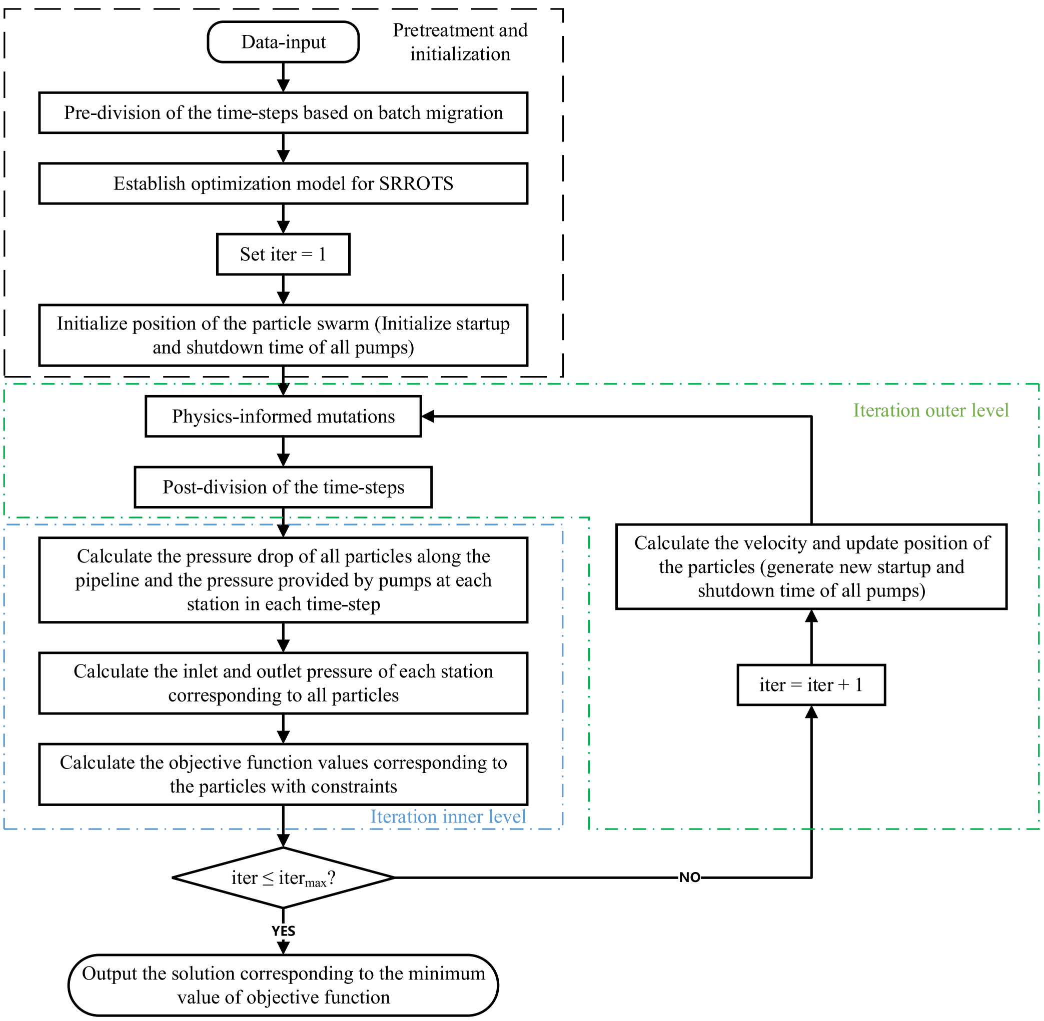

FIGURE 5 | Flow chart of proposed PI-PSO algorithm.

29952166, 0, Downloaded from https://ietresearch.onlinelibrary.wiley.com/doi/10.1049/ein2.12024 by Welsh Assembly Government, Wiley Online Library on [06/05/2025]. See the Terms and Conditions (https://onlinelibrary.wiley.com/terms-and-conditions) on Wiley Online Library for rules of use; OA articles are governed by the applicable Creative Commons License

post-divided time-steps. Consequently, the inlet and outlet pressures at each station along the pipeline can be calculated, and the objective function, serving as the fitness function, can be obtained.

4.2.3 | Particle Initialising

The startup and shutdown times of the pumps, that is, $T^{S}_{i,k,m_{i,k}}$ and $T^{E}_{i,k,m_{i,k}}$, are considered as the dimensions of a particle's position as shown in Figure 8. Based on industrial experience on-site, the total number m of a pump's working time zones is 5. Before the iteration process, the positions and velocities of the particle swarm should be randomly initialised within the feasible domain.

4.3 | Iteration Process

4.3.1 | Physics-Informed Mutations

To ensure each particle's position is effective and realistic as much as possible, physics-informed mutations are essential.

XXX Energy Company

Notice of Sequential Pipeline Transmission Plan in February 2024

No.: 202402-01

(Line 1)

No.	St.	Start time	End time	Batch No.	Liquid type	Total mass (10kton)	Total volume (10km3)	Flowrate (m3/h)	Flowrate (t/h)	Note
1	NS	2024/2/10 6:00	2024/2/10 15:51	G-005	95# Gasoline	0.292	0.39	400	296	0.90
2	NS	2024/2/10 15:51	2024/2/10 16:42	G-005	95# Gasoline	0.022	0.03	350	259	
3	NS	2024/2/10 16:42	2024/2/11 8:30	G-005	95# Gasoline	0.538	0.73	460	340	
4	NS	2024/2/11 8:30	2024/2/11 10:21	G-005	95# Gasoline	0.048	0.06	350	259	
6	NS	2024/2/11 10:21	2024/2/11 11:12	G-003	92# Gasoline	0.022	0.03	350	259	2.57
7	NS	2024/2/11 11:12	2024/2/12 11:01	G-003	92# Gasoline	0.811	1.10	460	340	
8	NS	2024/2/12 11:01	2024/2/12 12:07	G-003	92# Gasoline	0.028	0.04	350	259	
9	NS	2024/2/12 12:07	2024/2/14 14:15	G-003	92# Gasoline	1.709	2.31	460	340	
10	SD	2024/2/10 6:00	2024/2/10 15:51	D-004	Bio diesel	0.14	0.17	171	142	

FIGURE 6 | A typical input data sheet by an energy company in China.

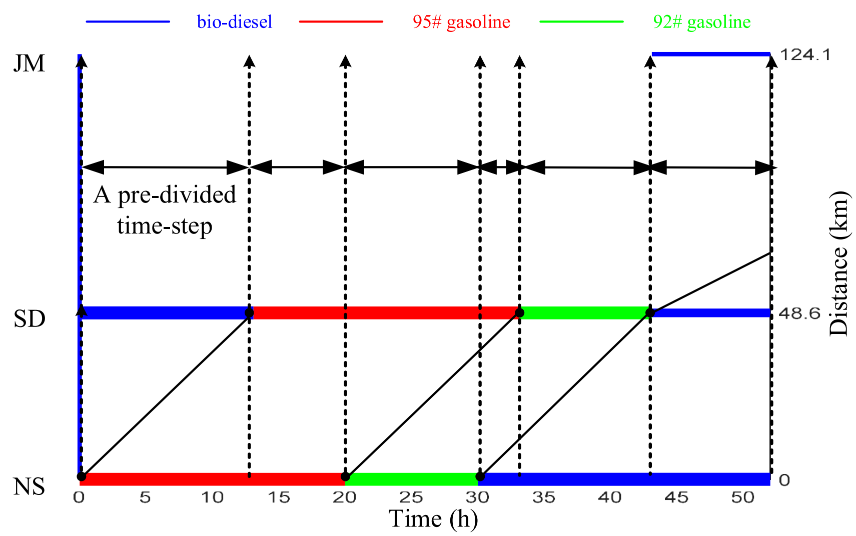

FIGURE 7 | Pre-division of the time-steps with the batch migration chart.

$$\overbrace{\left[T^{S}_{1,1,1},T^{E}_{1,1,1},T^{S}_{1,1,2},T^{E}_{1,1,2},\cdots,T^{S}_{1,2,1},T^{E}_{1,2,1},\cdots,T^{S}_{2,1,1},\cdots T^{S}_{i,k,1},\cdots,T^{S}_{i,k,m},\cdots,T^{S}_{i_{\max},k_{i_{\max}},m},T^{E}_{i_{\max},k_{i_{\max}},m}\right]}^{\text{Number of dimensions in a particle: } \sum_{i\in I} k_{i_{\max}} \times m \times 2}$$

FIGURE 8 | Schematic diagram of a particle's composition.

29952166, 0, Downloaded from https://ietresearch.onlinelibrary.wiley.com/doi/10.1049/ein2.12024 by Welsh Assembly Government, Wiley Online Library on [06/05/2025]. See the Terms and Conditions (https://onlinelibrary.wiley.com/terms-and-conditions) on Wiley Online Library for rules of use; OA articles are governed by the applicable Creative Commons License

These mutations involve four sequential steps, which accelerate both convergence and the search for the optimal solution. The mutation process is illustrated in Figure 9, with numbers in parentheses corresponding to the respective steps. To enhance clarity, step (2) is presented twice. The detailed process of physics-informed mutations is as follows:

1. Rank the startup and shutdown times

Due to the random operations involved in the generation and update processes of particles, there is a possibility that a pump's startup time could be later than its shutdown time. Therefore, it is necessary to swap the startup and shutdown times of any pump for which this condition occurs.

2. Remove the overlap time of a pump's working time zones

Also due to the random operations involved in the generation and update of particles, it is possible for a pump's working time zones to overlap, which is impractical. Therefore, the overlap time should be considered only in one working time zone and eliminated from the others. The working time zone in which the overlap time is retained is chosen randomly.

3. Sequence the pump's working time zones

There is a possibility that the five time periods of a pump do not follow a chronological order, which is impractical. Therefore, the pump's working time zones should be sequenced.

4. Split the pump's working time zones

If, in a certain iteration, a pump runs for the entire scheduling horizon, its corresponding working time zones will be evenly divided into five parts and distributed across five time periods.

By following the steps of the physics-informed mutations, the pump running time becomes practical and can be utilised to calculate the objective function and pressure distribution.

4.3.2 | Calculating the Objective Function and Pressure Distribution

Before calculating the objective function and pressure distribution, the time-steps must be post-divided. In these post-divided time-steps, the status of each pump remains stable. The pressure distribution calculation is twofold. First, the pressure drop of all particles along the pipeline and the pressure provided by pumps at each station within each time-step are calculated. Then, the inlet and outlet pressures at each station corresponding to all particles are evaluated. After calculating the pressure distribution, the objective function values for particles are obtained.

4.3.3 | Iterations

If the iteration number $\text{iter} \le \text{iter}_{\max}$, the iteration continues until it reaches its maximum number. After each iteration, the position and velocity of the particle swarm are updated according to the equations below:

$$\begin{aligned} v_{o,d}^{\text{iter}+1} &= w \cdot v_{o,d}^{\text{iter}} + c_1 \cdot \text{rand}() \cdot \left(p_{o,d} - x_{o,d}^{iter}\right) \\ &\quad + c_2 \cdot \text{rand}() \cdot \left(p_{\text{gbest}} - x_{o,d}^{\text{iter}}\right) \\ x_{o,d}^{\text{iter}+1} &= x_{o,d}^{\text{iter}} + v_{o,d}^{\text{iter}+1} \quad o = 1, 2, \cdots, O; d = 1, 2, \cdots, D \end{aligned} \tag{29}$$

where o represents the oth particle in the particle swarm and O is the population of particle; d represents the dth dimension of a particle and D is the number of dimensions in a particle which is presented in Figure 8; $v_{o,d}^{\text{iter}}$ and $x_{o,d}^{\text{iter}}$ are the velocity and

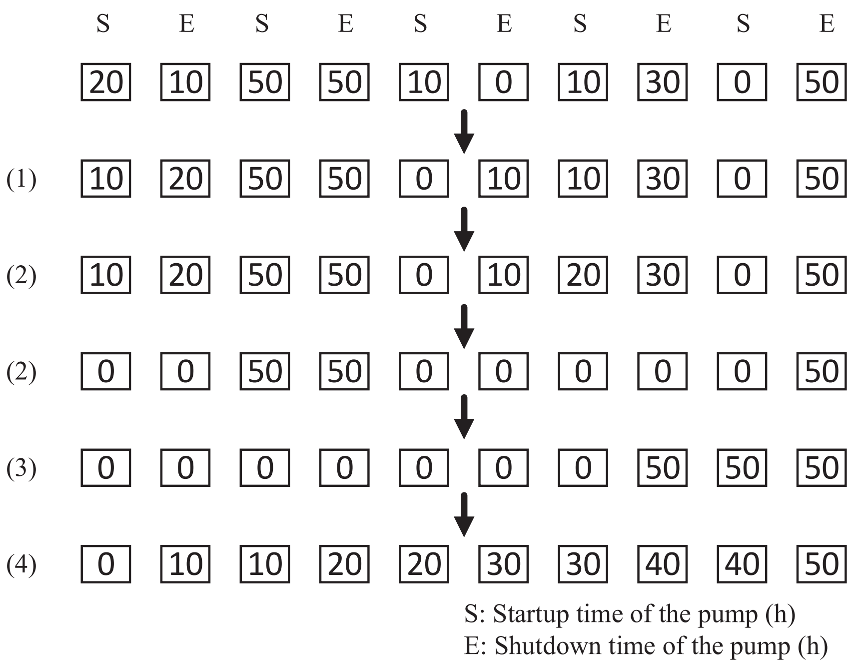

FIGURE 9 | Sketch map of physics-informed mutations.

29952166, 0, Downloaded from https://ietresearch.onlinelibrary.wiley.com/doi/10.1049/ein2.12024 by Welsh Assembly Government, Wiley Online Library on [06/05/2025]. See the Terms and Conditions (https://onlinelibrary.wiley.com/terms-and-conditions) on Wiley Online Library for rules of use; OA articles are governed by the applicable Creative Commons License

position of the dth dimension of the oth particle in the iterth iteration, respectively; $p_{o,d}$ is the best position (i.e., with the local minimum objective function value) of the dth dimension of the oth particle in all the previous iterations; p_{gbest} is the best position of the particle with the minimum objective function value in the particle swarm in the current iteration; w is the inertia weight representing the effect of the velocity in the current iteration to the next iteration; c_1 and c_2 are acceleration factors that work with a random number whose mathematical expectation is 0.5. These factors adjust the influence of the deviation between the current position of the particle and the current best position of the particle swarm, as well as the deviation between the current position of the particle and its best position in all previous iterations. Note that the randomisation operations during the update and mutation processes can enhance the convergence of the algorithm and facilitate finding the optimal solution. At the end of the iteration, the solution corresponding to the minimum value of the objective function is output.

5 | Case Studies

In this section, both an illustrative SRROTS and a real-world SRROTS in South China are utilised to validate the proposed continuous-time optimal energy management model and the corresponding PI-PSO algorithm. The configuration of the illustrative system is shown in Figure 10. Detailed batch delivery information and local demands are displayed, achieving a load balance among the IS, LS, and TSs. Parameters relating to the product types [32], pumps and pipelines are provided in Table 2, Tables 3 and 4. Note that the SRROTS is initially filled with gasoline. For the PI-PSO algorithm, the inertia weight w is set to 0.9, the acceleration factors c_1 and c_2 are both set to 2, and the maximum iteration number is 400. For other parameters, $\text{Pen}^{\text{status}}$ and Pen^{safe} are set to 1000 kWh and 100 kWh/(Pa·h), respectively.

5.1 | Necessity of the Proposed Model

To demonstrate the necessity of the proposed model for operational safety, we compare the following two cases, each representing a different model for the energy management of SRROTSs.

Case 1: the proposed model with T_N variable time-steps by proposed PI-PSO algorithm.

Case 2: the traditional model with T_N equally-divided time-steps by solvers.

A comparative result between the proposed model and traditional model with $T_N = 10$ is shown in Figure 11. According to the results, PIS1-3 provides a pumping head of 277.73 m, which is approximately half of PLS1-3's 462.41 m. The proposed model accurately determines the exact time to switch the electric pumps at 36.73 h, ensuring no safety issues with pressure distribution at any time or location. Note that a pressure of zero indicates that the station and its upstream pipeline are not operational at that time and, therefore, are not constrained by pressure limits. In contrast, the traditional model fails to adjust pump operations promptly, resulting in pressure falling below the limit (as displayed in the red rectangle in Figure 11d). The issue arises because the time-steps are equally divided without considering the physical characteristics of SRROTSs, allowing parameters to change suddenly within a time-step. As a result, the changing tendencies over time cannot be fully captured, leading to model distortion and an inaccurate operation schedule. A further comparative analysis on the objective value and CPU time of the different models is given in Table 5. Conclusions are drawn. The proposed model achieves optimal energy management of the SRROTS in 21.47 s, using 18 time-steps to accurately determine the exact pump switching times. For traditional models, fewer divisions result in shorter CPU times but lower accuracy, potentially leading to safety issues. Conversely, more divisions lead to excessively long computation times (two orders of magnitude higher than the proposed model), although the accuracy is comparable to that of the proposed methods. Hence, the proposed model effectively balances accuracy and solution time, which is necessary for on-site usage, ensuring operational safety.

Interestingly, it is observed from Table 5 that as the number of divisions T_N increases, the operational energy consumption f_1 does not necessarily increase. To illustrate this issue, we discuss three scenarios when T_N increases. As illustrated in Figure 12a, when a time-step is further divided and the pressure at both its start and end times satisfies the pressure constraints, the

TABLE 2 | Physical properties of liquid products.

Product types	Density (kg/m^3)	Kinetic viscosity (m^2/s)
92# gasoline	724	2×10^{-6}
Bio-diesel	847.4	6×10^{-6}

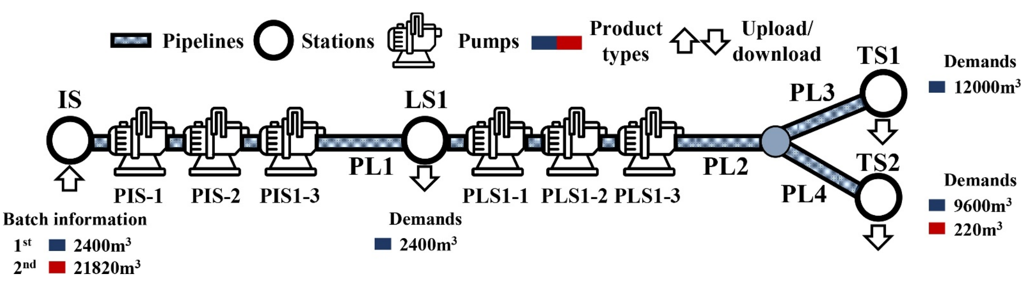

FIGURE 10 | Configuration of the illustrative SRROTS.

29952166, 0, Downloaded from https://ietresearch.onlinelibrary.wiley.com/doi/10.1049/ein2.12024 by Welsh Assembly Government, Wiley Online Library on [06/05/2025]. See the Terms and Conditions (https://onlinelibrary.wiley.com/terms-and-conditions) on Wiley Online Library for rules of use; OA articles are governed by the applicable Creative Commons License

TABLE 3 | Pump characteristics coefficients.

Pump no.	$a_{i,k}$,	$b_{i,k}$	$m_{i,k}$	$a_{0i,k}$	$a_{1i,k}$	$b_{1i,k}$
PIS1-1	−2.7e-4	1.975	263.6	55.63	−28.08	15.88
PIS1-2	−2.2e-4	1.975	300.5	55.69	−24.02	18.20
PIS1-3	−4.0e-4	1.886	300.7	6.432	−15.68	91.99
PLS1-1	−2.9e-4	2.365	360.1	67.71	−8.001	−14.57
PLS1-2	−9.1e-6	2.602	497.0	17.52	−23.67	73.51
PLS1-3	−9.1e-6	2.603	496.1	36.57	−29.17	44.56
Pump no.	$a_{2i,k}$	$b_{2i,k}$	$a_{3i,k}$	$b_{3i,k}$	$\omega_{i,k}$	$Q_{t,i,min/max}^{pump}$
PIS1-1	−3.355	5.939	5.939	5.939	0.005529	100/700
PIS1-2	−2.095	5.427	5.427	5.427	0.004711	50/700
PIS1-3	17.93	7.263	7.263	7.263	0.003200	50/700
PLS1-1	1.469	−4.953	−4.953	−4.953	0.02100	50/300
PLS1-2	13.09	7.111	7.111	7.111	0.004498	50/600
PLS1-3	5.493	8.027	8.027	8.027	0.005178	100/600

TABLE 4 | Pipeline design parameters.

St./Pipe. No.	$P\ IN_{min}$	$P\ IN_{max}$	$P\ OUT_{min}$	$P\ OUT_{max}$	L_i	Z_i	D_i
IS/PL1	0.7	7	0.1	4.8	65,494	12.76	0.3556
LS1/PL2	0.7	4.5	0.1	8.7	79,681	53.58	0.3556
TS1/PL3	0.7	5.5	/	/	28,292	−77.38	0.3239
TS2/PL4	2.5	5.5	/	/	75,010	−56.19	0.3556

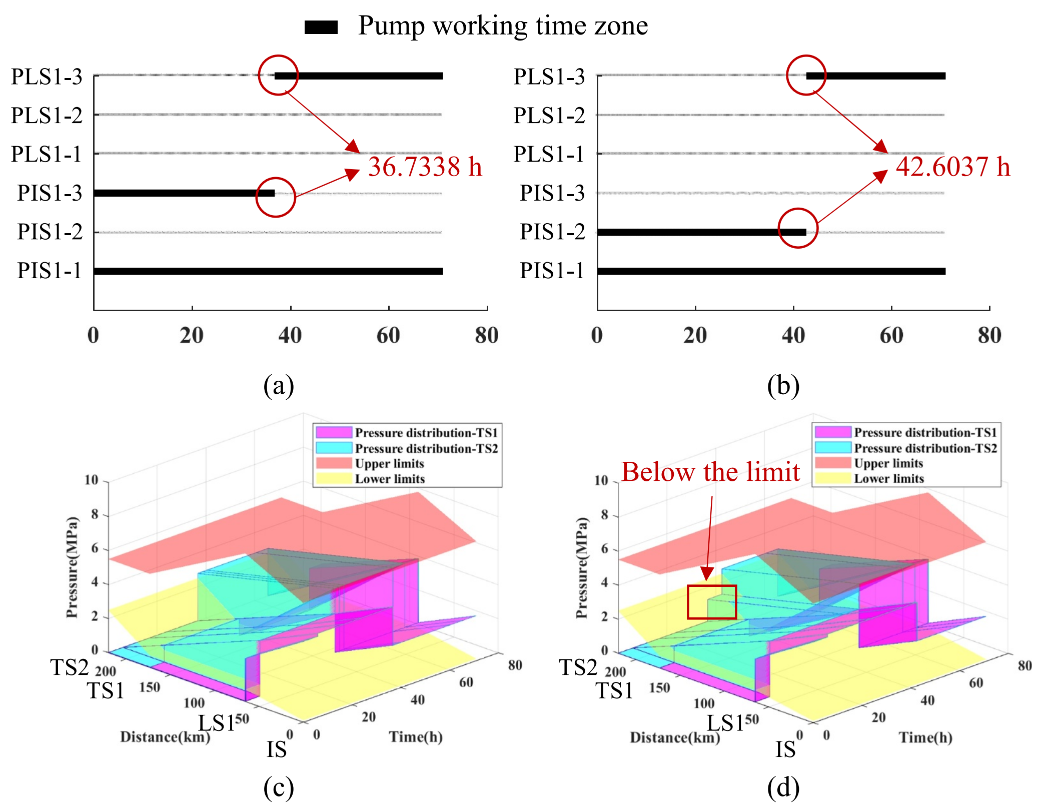

FIGURE 11 | Comparison of energy management result in the illustrative SRROTS. (a) Pump schedule in Case 1. (b) Pump schedule in Case 2. (c) Temporal-spatial pressure distribution in Case 1. (d) Temporal-spatial pressure distribution in Case 2 ($\boldsymbol{T_N} = \mathbf{10}$).

29952166, 0, Downloaded from https://ietresearch.onlinelibrary.wiley.com/doi/10.1049/ein2.12024 by Welsh Assembly Government, Wiley Online Library on [06/05/2025]. See the Terms and Conditions (https://onlinelibrary.wiley.com/terms-and-conditions) on Wiley Online Library for rules of use; OA articles are governed by the applicable Creative Commons License

TABLE 5 | Comparative results of different models in the illustrative SRROTS.

Method	T_N	Objective value (kWh)				CPU time (s)
		Obj	f_1	$f_{\text{on-off}}$	f_{safe}	
Proposed model	**18**	**45,356.55**	**43,356.55**	**2000**	**0**	**21.47**
Traditional model	10	10,085,261,48.15	42,351.76	2000	1,008,481,796.39	0.70
	100	36,522,769.37	43,323.25	2000	36,477,446.12	12.51
	500	12,222,682.31	43,344.95	2000	12,177,337.36	374.88
	1000	45,356.72	43,356.72	2000	≈ 0	2336.11

Note: The bold values are to highlight the superior performance of the proposed method.

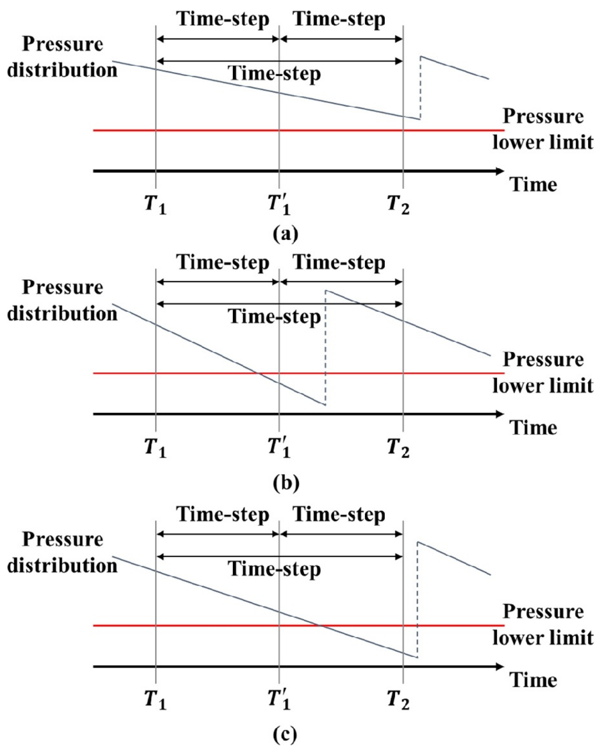

FIGURE 12 | Three scenarios when further equally dividing the time-steps. (a) Scenario 1: the objective value remains unchanged. (b) Scenario 2: the objective value increases. (c) Scenario 3: the objective value decreases.

objective value remains unchanged if the pressure at newly added division points also meets these conditions; otherwise, the objective value will increase as depicted in Figure 12b. When a time-step is further divided and the pressure at one of its start and end times does not satisfy the pressure constraints, such as in Figure 12c, the objective value will decrease if pressure at the newly added division points meets the limits.

5.2 | Performance of the Proposed PI-PSO Algorithm

To better illustrate the performance of the proposed PI-PSO algorithm, comparisons with other popular metaheuristic variations are conducted based on Case 1:

A. the proposed model with similarity-based algorithm [33].

B. the proposed model with diversity-based algorithm [34].

C. the proposed model with original PSO algorithm [35].

The detailed results for the numerical test of different algorithms are depicted in Figure 13. The iteration evolutions in Figure 13a demonstrate that the proposed PI-PSO algorithm achieves the best performance regarding the objective value, although it requires slightly more iterations to reach convergence. In contrast, the original PSO algorithm performs the worst, converging at an early stage with an objective value 25.6% higher than that of the proposed method. The similarity-based algorithm and diversity-based algorithm rank second and third in terms of objective value performance, respectively. There is a trade-off between improving the objective value and the number of iterations needed for convergence. However, given that the scheduling horizon is much longer than the iteration time, the proposed PI-PSO algorithm remains valuable and promising. The temporal-spatial pressure distribution in Case 1a, 1b and 1c are shown in Figure 13b–d, respectively. Additionally, the proposed method is entirely free of solvers, making it easy to implement on-site to address potential energy security issues.

Given that metaheuristic methods rely on random operations, discrepancies between the results of each calculation are possible. Therefore, it is important to evaluate metrics such as the average objective value, average convergence iteration number, and average convergence time to effectively demonstrate the performance of the proposed method. The results are given in Table 6, where 1000 repeated calculations are conducted. Comparatively, the PI-PSO algorithm is the most stable in solution performance, although it requires more convergence time. The results align with the tendencies observed in the aforementioned analysis, further confirming the superior performance of the proposed PI-PSO algorithm.

5.3 | Test on a Real-World SRROTS in South China

A modified real-world SRROTS in South China is used to further verify the scalability of the proposed model and the PI-PSO algorithm. The system configuration is shown in Figure 14. It spans a total length of 285.85 km, with 6 pipelines and 3

29952166, 0, Downloaded from https://ietresearch.onlinelibrary.wiley.com/doi/10.1049/ein2.12024 by Welsh Assembly Government, Wiley Online Library on [06/05/2025]. See the Terms and Conditions (https://onlinelibrary.wiley.com/terms-and-conditions) on Wiley Online Library for rules of use; OA articles are governed by the applicable Creative Commons License

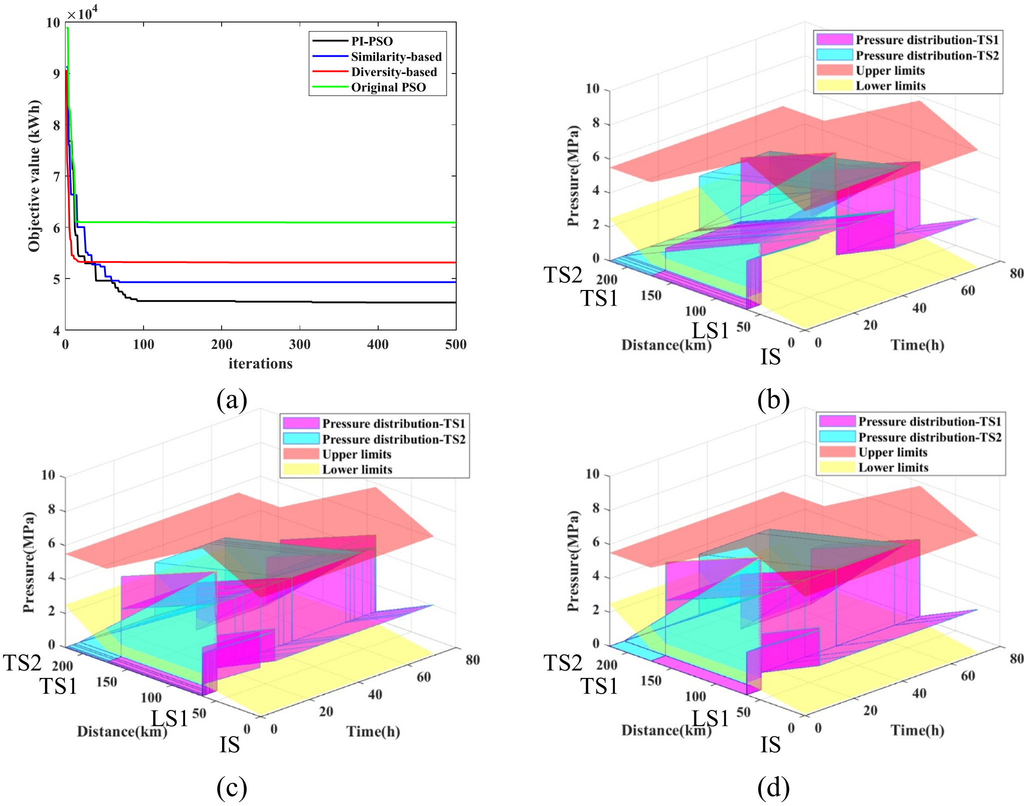

FIGURE 13 | Results of different algorithms. (a) Iteration evolutions. (b) Temporal-spatial pressure distribution in Case 1a. (c) Temporal-spatial pressure distribution in Case 1b. (d) Temporal-spatial pressure distribution in Case 1c.

TABLE 6 | Comparative metrics of different algorithms on the illustrative SRROTS.

Method	Proposed PI-PSO	Similarity-based	Diversity-based	Original PSO
Averaged objective value (kWh)	**45,396.33**	49,519.48	51,328.13	57,796.29
Maximum objective value (kWh)	**47,810.07**	59,004.85	60,485.44	101,027.40
Minimum objective value (kWh)	**45,356.55**	45,699.50	46,267.40	50,309.68
Averaged convergence iteration number	395.41	310.46	301.19	269.56
Averaged convergence time (s)	23.60	21.18	13.43	13.34

Note: The bold values are to highlight the superior performance of the proposed method.

pumping stations (a total of 8 pumps), supplying oil to an area of 18,486 km^2. Additional detailed parameters can be accessed from [10, 36].

The results of the proposed model using the PI-PSO algorithm are illustrated in Figure 15. In Figure 15a, the detailed upload and download flow rates of different product types at each station are shown. The pump scheduling results are displayed in Figure 15b,c provides the corresponding system's temporal-spatial pressure distribution. Finally, the iteration evolutions are depicted in Figure 15d. Overall, the PI-PSO algorithm effectively solves the proposed model with good scalability for real-world SRROTS. However, it requires more convergence iterations when dealing with larger-scale problems. Additionally, compared to the similarity-based algorithm, it achieves a 6.63% improvement in the objective value, reducing energy consumption by 18,123.67 kWh. If applied to SRROTSs across South and West China, where approximately 310 million kWh are annually consumed, this could result in an annual reduction of 20.553 million kWh in energy consumption, equivalent to 13,110.76 tons of CO_2 emission reduction per year (0.6379 $kgCO_2/kWh$ in China in 2023 [37]). Consequently, the proposed continuous-time optimal energy management model and the PI-PSO algorithm are crucial for the safe and low-carbon operation of SRROTSs and have the potential for application in other pipeline transmission systems, such as crude oil pipelines and urban water distribution systems.

6 | Conclusions and Perspectives

This paper focuses on the energy management of the emerging shared renewables and refined oil transmission systems

29952166, 0, Downloaded from https://ietresearch.onlinelibrary.wiley.com/doi/10.1049/ein2.12024 by Welsh Assembly Government, Wiley Online Library on [06/05/2025]. See the Terms and Conditions (https://onlinelibrary.wiley.com/terms-and-conditions) on Wiley Online Library for rules of use; OA articles are governed by the applicable Creative Commons License

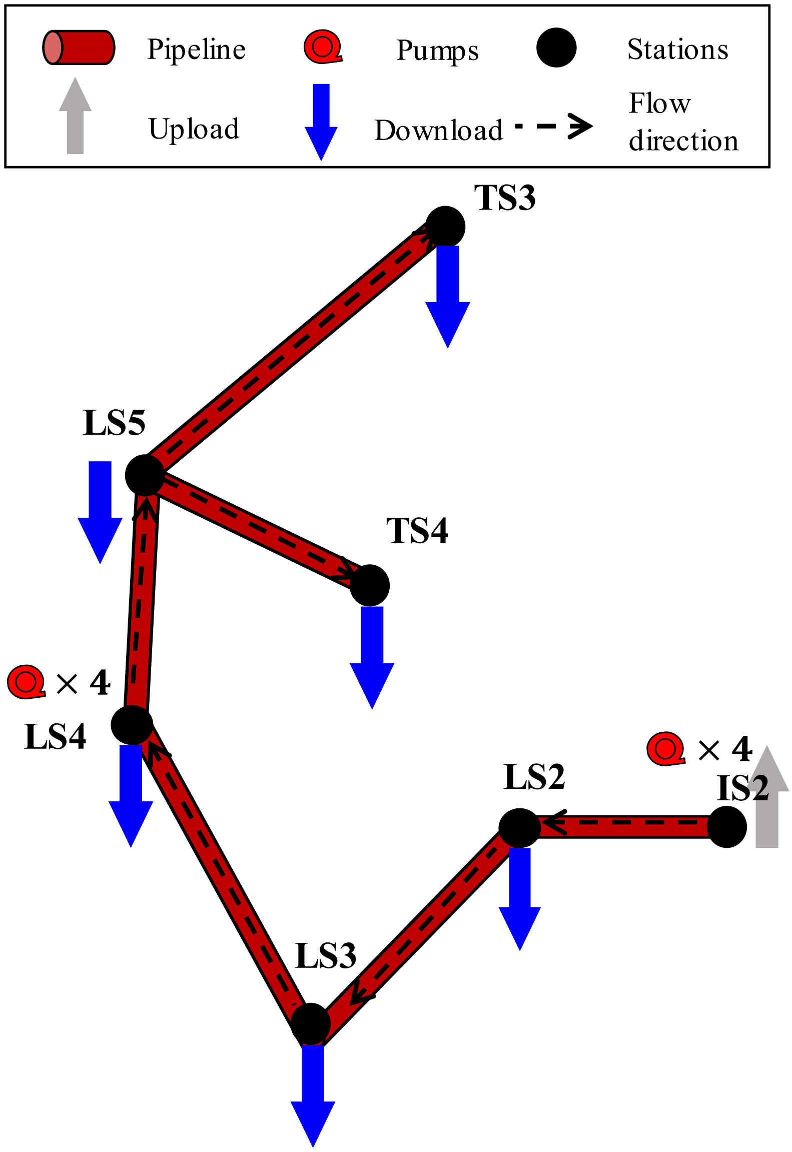

FIGURE 14 | Configuration of the modified real-world SRROTS in South China.

(SRROTSs) in the energy transition and also addresses its safety issues. Conclusions are drawn as follows:

1. The proposed continuous-time energy management model effectively balances accuracy and solution time, crucial for on-site usage, ensuring safe and efficient operation in SRROTSs. For a system with 4 pipelines, it achieves the optimal solution in just 21.47 s.

2. The proposed physics-informed particle swarm optimisation (PI-PSO) algorithm demonstrates superior optimality and stability compared to other popular algorithm variations. Specifically, it achieves a 25.6% energy reduction compared to the original PSO algorithm. It is observed that there is a trade-off between improving the objective value and the number of iterations needed for convergence. Additionally, the proposed method is entirely free of solvers, making it easy to implement on-site to address potential energy security issues.

3. The scalability of the proposed model and the PI-PSO algorithm has been verified on a real-world SRROTS in South China. The PI-PSO algorithm effectively solves the proposed model for these systems, although it requires more convergence iterations when dealing with larger-scale problems. It is estimated that SRROTSs across South and West China can achieve a reduction of 13,110.76 tons of CO_2 emissions per year.

However, we acknowledge that local optima can sometimes occur when using the PI-PSO algorithm. To enhance its performance, it is essential to deepen our understanding of the physical system, particularly the empirical operation schemes on-site, and embed this knowledge into the algorithm's design. This will be the focus of our future work.

29952166, 0, Downloaded from https://ietresearch.onlinelibrary.wiley.com/doi/10.1049/ein2.12024 by Welsh Assembly Government, Wiley Online Library on [06/05/2025]. See the Terms and Conditions (https://onlinelibrary.wiley.com/terms-and-conditions) on Wiley Online Library for rules of use; OA articles are governed by the applicable Creative Commons License

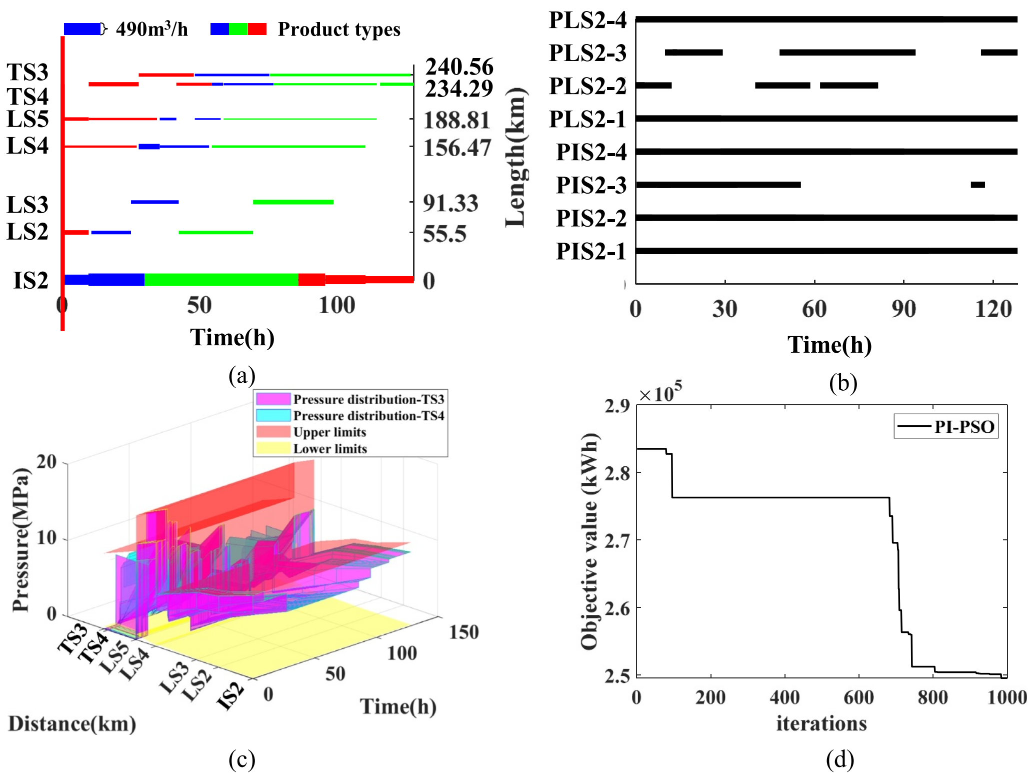

FIGURE 15 | Energy management result of the real-world SRROTS. (a) Batch schedule. (b) Pump schedule. (c) Temporal-spatial pressure distribution. (d) Iteration evolutions.

Nomenclature

Index sets

Indices	Description
$t \in T = \{1, 2 \ldots t_{\max}\}$	Set of time-steps
$i \in I = \{1, 2 \ldots i_{\max}\}$	Set of stations
$k \in K_i = \{1, 2 \ldots k_{i\max}\}$	Set of pumps in station i
$b \in B = \{1, 2 \ldots b_{\max}\}$	Set of batches
$b^s_{t,i} \in B^s_{t,i} = \{1, 2 \ldots b^s_{t,i,\max}\}$	Set of batches within pipeline segment $(i, i+1)$ during time-step t

Continuous parameters

Parameters	Description	Unit
$\rho_{t,i}$	Density of the liquid products flowing through station i in time-step t	kg/m^3
G	Gravitational acceleration	m/s^2
$Q^{\text{pump}}_{t,i}$	Flow rate through station i during time-step t	m^3/h
$Q^{\text{segment}}_{t,i}$	Flow rate through pipeline segment $(i, i+1)$ during time-step t	m^3/h
$TS_{i,k}$	Minimum startup/shutdown time of pump k at station i	h
$\text{Pen}^{\text{status}}$	Penalty coefficient of pumps' startup/shutdown	kWh

(Continues)

(Continued)

Parameters	Description	Unit
Pen^{safe}	Penalty coefficient of safety issues	kWh/(MPa·h)
$H_{t,i,k}$	Pumping head of pump k at station i during time-step t	m
$\eta_{t,i,k}$	Efficiency of pump k at station i during time-step t	%
$a_{i,k}, b_{i,k}, m_{i,k}$	Pumping head coefficients of pump k at station i	/
$a_{0i,k}, a_{1i,k}, b_{1i,k}, a_{2i,k}, b_{2i,k}, a_{3i,k}, b_{3i,k}, \omega_{i,k}$	Efficiency coefficients of pump k at station i	/
M	A sufficiently large number	/
P^f_t	Pressure provided by feed pumps in time window t	MPa
D_i	Internal diameter of segment $(i, i+1)$	m
$\rho_{t,i,b^s_{t,i}}$	Density of the liquid product batch $b^s_{t,i}$ within pipeline segment $(i, i+1)$ during time-step t	kg/m^3
$\lambda_{t,i,b^s_{t,i}}$	Friction factor of the liquid product batch $b^s_{t,i}$ within pipeline segment $(i, i+1)$ during time-step t	/
L_i, Z_i	Length and elevation of station i	m
θ_i	Dip angle of pipeline segment $(i, i+1)$	°
$P\,\text{IN}_{\min}$	Minimum inlet pressure of station i	MPa
$P\,\text{IN}_{\max}$	Maximum inlet pressure of station i	MPa

(Continues)

29952166, 0, Downloaded from https://ietresearch.onlinelibrary.wiley.com/doi/10.1049/ein2.12024 by Welsh Assembly Government, Wiley Online Library on [06/05/2025]. See the Terms and Conditions (https://onlinelibrary.wiley.com/terms-and-conditions) on Wiley Online Library for rules of use; OA articles are governed by the applicable Creative Commons License

(Continued)

Parameters	Description	Unit
$P\ OUT_{min}$	Minimum outlet pressure of station i	MPa
$P\ OUT_{max}$	Maximum outlet pressure of station i	MPa
$\alpha_{t,i}$, $\beta_{t,i}$	Coefficients of the equation between time and pressure drop of pipeline segment $(i, i+1)$ during time-step t	/
$Q^{pump}_{t,i,min}$	Minimum flow rate through pump k at station i	m^3/h
$Q^{pump}_{t,i,max}$	Maximum flow rate through pump k at station i	m^3/h

Continuous variables

Variables	Description	Unit
$P_{t,i,k}$	Power of pump k at station i during time-step t	kW
$P^{station}_{t,i}$	Pressure provided by station i during time-step t	MPa
TP_t	Length of time-step t	h
$\mathrm{PIN}_{t,i}/PI_{t,i}$	Inlet pressure of station i at the start/end time of time-step t	MPa
$\mathrm{POUT}_{t,i}/PO_{t,i}$	Outlet pressure of station i at the start/end time of time-step t	MPa
$P^{drop}_{t,i}$	Pressure drop of pipeline segment $(i, i+1)$ at the start time of time-step t	MPa
$\delta^{pressure,1/2/3/4}_{t,i,min/max}$	Auxiliary variables of pipeline segment $(i, i+1)$ during time-step t	MPa

Binary variables

Variables	Description	Unit
$SP_{t,i,k}$	If pump k at pump station i is on during time-step t, $SP_{t,i,k} = 1$, otherwise, $SP_{t,i,k} = 0$	/
$SA_{t,i,k}$	If the startup/shutdown status of pump k at station i during time-step t is different with that of its previous time-step, $SA_{t,i,k} = 1$, otherwise $SA_{t,i,k} = 0$	/

Author Contributions

Shengshi Wang: conceptualization, methodology, software, writing – original draft, writing – review and editing, validation, visualization, formal analysis, data curation, investigation. **Danji Huang:** writing – review and editing, conceptualization, resources. **Jiakun Fang:** supervision, project administration, writing – original draft, writing – review and editing. **Xiaomeng Ai:** supervision, writing – original draft, writing – review and editing. **Shichang Cui:** writing – review and editing, writing – original draft. **Miao Li:** resources, funding acquisition. **Ge Yan:** resources, funding acquisition. **Kun Mei:** software, data curation, resources. **Sen Li:** data curation, investigation. **Qicong Liu:** software. **Hao Li:** software, data curation, investigation.

Conflicts of Interest

The authors declare no conflicts of interest.

Data Availability Statement

The data that support the findings of this study are available on request from the corresponding author. The data are not publicly available due to privacy or ethical restrictions.

References

1. Y. Li, X. Yang, E. Du, et al. "A Review on Carbon Emission Accounting Approaches for the Electricity Power Industry," *Applied Energy* 359 (2024): 122681, https://doi.org/10.1016/j.apenergy.2024.122681.

2. Z. Liu, Z. Deng, S. J. Davis, and P. Ciais, "Global Carbon Emissions in 2023," *Nature Reviews Earth & Environment* 5, no. 4 (2024): 253–254, https://doi.org/10.1038/s43017-024-00532-2.

3. R. Tu, H. Zhang, S. Xu, et al. "Pipeline Sharing: Boosting Multi-Product Pipeline Transport Biofuels in the Shift to Low-Carbon Energy," *Journal of Cleaner Production* 437 (2024): 140663, https://doi.org/10.1016/j.jclepro.2024.140663.

4. W. Zhao, Q. Liao, R. Qiu, et al. "Pipe Sharing: A Bilevel Optimization Model for the Optimal Capacity Allocation of Natural Gas Network," *Applied Energy* 359 (2024): 122731, https://doi.org/10.1016/j.apenergy.2024.122731.

5. G. Ren, J. Wan, J. Liu, and D. Yu, "Spatial and Temporal Assessments of Complementarity for Renewable Energy Resources in China," *Energy* 177 (2019): 262–275, https://doi.org/10.1016/j.energy.2019.04.023.

6. R. Tu, C. Liu, Qi Shao, Qi Liao, R. Qiu, and Y. Liang, "Pipeline Sharing: Optimal Design of Downstream Green Ammonia Supply Systems Integrating With Multi-Product Pipelines," *Renew Energy* 223 (2024): 120024, https://doi.org/10.1016/j.renene.2024.120024.

7. Z. Li, Y. Liang, Qi Liao, N. Xu, J. Zheng, and H. Zhang, "Scheduling of a Branched Multiproduct Pipeline System With Robust Inventory Management," *Computers & Industrial Engineering* 162 (2021): 107760, https://doi.org/10.1016/j.cie.2021.107760.

8. S. Wang, J. Fang, J. Wu, et al. "Learning-Based Spatially-Cascaded Distributed Coordination of Shared Transmission Systems for Renewable Fuels and Refined Oil With Quasi-Optimality Preservation Under Uncertainty," *Applied Energy* 381 (2025): 125085, https://doi.org/10.1016/j.apenergy.2024.125085.

9. M. Sidki, N. Tchernev, P. Féniès, L. Ren, and S. Elfirdoussi, "Multi-product Pipeline Scheduling: A Comprehensive Bibliometric Analysis and a Systematic Literature Review," *Computers & Chemical Engineering* 192 (2024): 108911, https://doi.org/10.1016/j.compchemeng.2024.108911.

10. S. Wang, J. Fang, X. Ai, et al. "Implementation and Field Test of Optimal Pump Scheduling in the Multi-Product Refined Oil Transmission System," *IEEE Transactions on Industry Applications* 58, no. 6 (2022): 1–12, https://doi.org/10.1109/tia.2022.3201558.

11. R. Tu, Qi Liao, N. Xu, et al. "Pipeline Sharing: Potential Capacity Analysis of Biofuel Transportation Through Existing Pipelines," *Journal of Cleaner Production* 398 (2023): 136507, https://doi.org/10.1016/j.jclepro.2023.136507.

12. S. Wang, H. Li, D. Huang, et al. "On Security-Constrained Bidding of Shared Transportation Hubs for Renewable Fuels and Refined Oil Participating Within Energy, Regulation and Pipeline Logistics Markets," in *2024 IEEE 7th Student Conference on Electric Machines and Systems (SCEMS)* (Macao, Macao: IEEE, 2024), 1–6.

13. R. Tu, Qi Liao, L. Huang, Y. Jiao, X. Wei, and Y. Liang, "Pipeline Sharing: Remaining Capacity Estimation of Multiproduct Pipelines," *Chemical Engineering Research and Design* 191 (2023): 338–352, https://doi.org/10.1016/j.cherd.2023.01.028.

14. R. Tu, C. Liu, Qi Shao, Qi Liao, R. Qiu, and Y. Liang, "Pipeline Sharing: Optimal Design of Downstream Green Ammonia Supply Systems Integrating With Multi-Product Pipelines," *Renew Energy* 223 (2024): 120024, https://doi.org/10.1016/j.renene.2024.120024.

29952166, 0, Downloaded from https://ietresearch.onlinelibrary.wiley.com/doi/10.1049/ein2.12024 by Welsh Assembly Government, Wiley Online Library on [06/05/2025]. See the Terms and Conditions (https://onlinelibrary.wiley.com/terms-and-conditions) on Wiley Online Library for rules of use; OA articles are governed by the applicable Creative Commons License

15. S. Wang, M. Li, B. Li, X. Ai, and J. Fang, "Optimal Operation of Integrated Power and Oil Transmission Systems," in *2021 IEEE 4th International Electrical and Energy Conference (CIEEC)* (Wuhan, China: IEEE, 2021), 1–6.

16. Qi Liao, Y. Liang, N. Xu, H. Zhang, J. Wang, and X. Zhou, "An MILP Approach for Detailed Scheduling of Multi-Product Pipeline in Pressure Control Mode," *Chemical Engineering Research and Design* 136 (2018): 620–637, https://doi.org/10.1016/j.cherd.2018.06.016.

17. Bo Zhou, J. Fang, X. Ai, W. Yao, and J. Wen, "Flexibility-Enhanced Continuous-Time Scheduling of Power System Under Wind Uncertainties," *IEEE Transactions on Sustainable Energy* 12, no. 4 (2021): 1–2320, https://doi.org/10.1109/tste.2021.3089696.

18. J. Liu, X. Ai, J. Fang, et al. "Continuous-Time Aggregation of Massive Flexible HVAC Loads Considering Uncertainty for Reserve Provision in Power System Dispatch," *IEEE Transactions on Smart Grid* 15, no. 5 (2024): 1–4849, https://doi.org/10.1109/tsg.2024.3398627.

19. Bo Zhou, X. Ai, J. Fang, et al. "Function-Space Optimization to Coordinate Multi-Energy Storage Across the Integrated Electricity and Natural Gas System," *International Journal of Electrical Power* 151 (2023): 109181, https://doi.org/10.1016/j.ijepes.2023.109181.

20. C. Zheng, J. Fang, S. Wang, X. Ai, Z. Liu, and Z. Chen, "Energy Flow Optimization of Integrated Gas and Power Systems in Continuous Time and Space," *IEEE Transactions on Smart Grid* 12, no. 3 (2021): 2611–2624, https://doi.org/10.1109/tsg.2020.3044609.

21. B. Zhou, R. Jiang, and S. Shen, "Frequency Stability-Constrained Unit Commitment: Tight Approximation Using Bernstein Polynomials," *IEEE Transactions on Power Systems* (2023).

22. K. I. Ibekwe, E. A. Etukudoh, Z. Q. S. Nwokediegwu, A. A. Umoh, A. Adefemi, and V. I. Ilojianya, "Energy Security in the Global Context: A Comprehensive Review of Geopolitical Dynamics and Policies," *Engineering Science & Technology Journal* 5, no. 1 (2024): 152–168, https://doi.org/10.51594/estj.v5i1.741.

23. S. Pfenninger, A. Hawkes, and J. Keirstead, "Energy Systems Modeling for Twenty-First Century Energy Challenges," *Renewable and Sustainable Energy Reviews* 33 (2014): 74–86, https://doi.org/10.1016/j.rser.2014.02.003.

24. J. Fang, Q. Zeng, X. Ai, Z. Chen, and J. Wen, "Dynamic Optimal Energy Flow in the Integrated Natural Gas and Electrical Power Systems," *IEEE Transactions on Sustainable Energy* 9, no. 1 (2018): 188–198, https://doi.org/10.1109/tste.2017.2717600.

25. L. Zuo, S. Wang, Y. Sun, et al. "Robustness Assessment of Wind Power Generation Considering Rigorous Security Constraints for Power System: A Hybrid RLO-IGDT Approach," *CSEE Journal of Power and Energy Systems* (2023).

26. Bo Zhou, X. Ai, J. Fang, et al. "Data-Adaptive Robust Unit Commitment in the Hybrid AC/DC Power System," *Applied Energy* 254 (2019): 113784, https://doi.org/10.1016/j.apenergy.2019.113784.

27. V. G. Cafaro, D. C. Cafaro, C. A. Méndez, and J. Cerdá, "MINLP Model for the Detailed Scheduling of Refined Products Pipelines With Flow Rate Dependent Pumping Costs," *Computers & Chemical Engineering* 72 (2015): 210–221, https://doi.org/10.1016/j.compchemeng.2014.05.012.

28. E. Osaba, E. Villar-Rodriguez, J. Del Ser, et al. "A Tutorial on the Design, Experimentation and Application of Metaheuristic Algorithms to Real-World Optimization Problems," *Swarm and Evolutionary Computation* 64 (2021): 100888, https://doi.org/10.1016/j.swevo.2021.100888.

29. S. Wang, L. Zuo, M. Li, et al. "The Data-Driven Modeling of Pressure Loss in Multi-Batch Refined Oil Pipelines With Drag Reducer Using Long Short-Term Memory (LSTM) Network," *Energies* 14, no. 18 (2021): 5871, https://doi.org/10.3390/en14185871.

30. E. Khlebnikova, K. Sundar, A. Zlotnik, R. Bent, M. Ewers, and B. Tasseff, "Optimal Economic Operation of Liquid Petroleum Products Pipeline Systems," *AIChE Journal* 67, no. 4 (2021): e17124, https://doi.org/10.1002/aic.17124.

31. J. Nayak, H. Swapnarekha, B. Naik, G. Dhiman, and S. Vimal, "25 Years of Particle Swarm Optimization: Flourishing Voyage of Two Decades," *Archives of Computational Methods in Engineering* 30, no. 3 (2023): 1663–1725, https://doi.org/10.1007/s11831-022-09849-x.

32. L. F. Ramírez Verduzco, "Density and Viscosity of Biodiesel as a Function of Temperature: Empirical Models," *Renewable and Sustainable Energy Reviews* 19 (2013): 652–665, https://doi.org/10.1016/j.rser.2012.11.022.

33. J. Kennedy and R. Eberhart, "Particle Swarm Optimization," *Proceedings of ICNN'95 - International Conference on Neural Networks* 4 (2002): 1942–1948, https://doi.org/10.1109/icnn.1995.488968.

34. D. Tian, Q. Xu, X. Yao, G. Zhang, Y. Li, and C. Xu, "Diversity-Guided Particle Swarm Optimization With Multi-Level Learning Strategy," *Swarm and Evolutionary Computation* 86 (2024): 101533, https://doi.org/10.1016/j.swevo.2024.101533.

35. W. Li, P. Liang, Bo Sun, Y. Sun, and Y. Huang, "Reinforcement Learning-Based Particle Swarm Optimization With Neighborhood Differential Mutation Strategy," *Swarm and Evolutionary Computation* 78 (2023): 101274, https://doi.org/10.1016/j.swevo.2023.101274.

36. S. Wang. SRROTS-data_sharing." ([dataset], 2024), Vol. v1, GitHub, https://github.com/datasharing4manuscript/SRROTS-data_sharing.git.

37. Website, "Does Guangdong Province Officially Release the Carbon Emission Factor of the Power Grid? (in Chinese)" (Guangzhou, China: Department of Ecology and Environment of Guangdong Province, 2024): [Online], https://gdee.gd.gov.cn/.

29952166, 0, Downloaded from https://ietresearch.onlinelibrary.wiley.com/doi/10.1049/ein2.12024 by Welsh Assembly Government, Wiley Online Library on [06/05/2025]. See the Terms and Conditions (https://onlinelibrary.wiley.com/terms-and-conditions) on Wiley Online Library for rules of use; OA articles are governed by the applicable Creative Commons License